Available online at www.sciencedirect.com
SCIENCE DIRECT
Superlattices and Microstructures 39 (2006) 185–192
Superlattices and Microstructures
www.elsevier.com/locate/superlattices

Effect of aluminium doping on zinc oxide thin films grown by spray pyrolysis

A. El Manouni[a,b], F.J. Manjón[b], M. Mollar[b], B. Marí[b,*], R. Gómez[c], M.C. López[d], J.R. Ramos-Barrado[d]

[a] *Departament de Physique, Université Hassan II-Faculté de Sciences et Technologie. Mohammedia, Boulevard Yasmina, BP-145, 20650, Morocco*
[b] *Departament de Física Aplicada, Universitat Politècnica de València, Camí de Vera s/n, E-46022 València, Spain*
[c] *Departament de Química Física i Institut Universitari d'Electroquímica, Universitat d'Alacant, Apartat 99, E-03080 Alacant, Spain*
[d] *Departament de Física Aplicada, Universidad de Málaga, Avenida de Cervantes, 2, E-29071 Málaga, Spain*

Available online 19 September 2005

Abstract

We report the structural, optical, and electrical characterization of aluminium-doped zinc oxide thin films grown by the spray pyrolysis method. We report the effect of Al concentration on the resistivity and on the X-ray diffraction, transmittance, photoluminescence and Raman scattering spectra of the films. The minimum resistivity is obtained for the sample with nominal Al concentration of 1%. An increase of the Al doping decreases the quality of the films. The loss of short-range order affects the photoluminescence and resistivity, although the optical transmittance is good, and the decrease of the long-range order affects X-ray diffraction and Raman spectra.

1. Introduction

Wide bandgap semiconductor materials have been the centre of various studies in the last decade, owing to their physical properties and numerous applications including

* Corresponding author. Tel.: +34 96 387 70 00x75250; fax: +34 96 387 71 89.
E-mail address: bmari@fis.upv.es (B. Marí).

0749-6036/$ - see front matter © 2005 Elsevier Ltd. All rights reserved.
doi:10.1016/j.spmi.2005.08.041

solar cells, displays, and short wavelength devices [1,2]. In particular, the technologies of GaN-based materials have made much progress recently [3–5]. Another II–VI wide gap semiconductor, zinc oxide (ZnO), with bandgap $E_g = 3.37$ eV at room temperature, has also been paid much attention [6–8]. Since the exciton binding energy of ZnO is about 60 meV [9], roughly three times larger than that of GaN, and the biexciton formation energy of ZnO is about 15 meV [10], also much larger than that of GaN, ZnO is considered to be a promising material for novel exciton-related devices.

Zinc oxide thin films are enjoying a great interest as transparent conductive oxides due to their electro-optical properties, high electro-chemical stability and absence of toxicity. ZnO is an n-type semiconductor with a hexagonal wurtzite structure [11,12]. The ZnO conductivity is well-known to originate from the ionization of zinc interstitials and oxygen vacancies, which act as donor levels [10]. Between the above-mentioned two mechanisms, the formation of carriers by the ionization of zinc interstitials has been acknowledged to be predominant in intrinsic ZnO crystals. Unlike non-stoichiometric ZnO films, impurity-doped ZnO films show stable electrical and optical properties. Among the ZnO films doped with group III elements such as barium, aluminium, gallium and indium, aluminium-doped zinc oxide (AZO) films show the lowest electrical resistivity and a good optical transmission in the visible and near-infrared regions [13–15].

Numerous AZO thin film deposition techniques have been employed: chemical vapour deposition (CVD) [16], radio-frequency magnetron sputtering [17], sol–gel process [18], pulsed laser deposition [19], electrodeposition [20] and spray pyrolysis [15,21]. Compared to the others, the latter technique has many advantages: it is easy, inexpensive, and well adapted for mass fabrication.

In this paper, we study the effect of aluminium doping concentration on the structural, electrical, and optical properties of AZO thin films deposited directly onto quartz and onto Pt/quartz substrates by spray pyrolysis.

2. Experimental

AZO thin films were deposited on either quartz or platinum/quartz substrates at a temperature of about 400 °C by a spray pyrolysis technique. Details of the deposition system and method are described elsewhere [22,23]. An aqueous solution composed of zinc dichloride ($ZnCl_2$) was used as the starting material and aluminium trichloride ($AlCl_3$) as the dopant source. The concentration of the solution was 10^{-2} M and the concentration of Al was varied between 1% and 4% in the initial solution. Humid air (or oxygen) was used as the carrier gas, and the spray rate of the solution was 30 ml/h. The temperature of the substrate and the carrier gas pressure were respectively 400 °C and 2 bar. The distance between the substrate and solution source was 15 cm. Spraying times of 20 min provided films with thicknesses about 200 nm. All deposition parameters were optimized.

The crystal structure was determined by high-resolution X-ray diffraction in the θ–2θ configuration with a copper anticathode (Cu Kα, 1.54 Å). The optical properties were investigated by photoluminescence (PL), optical transmission, and Raman spectroscopy. Experimental systems for the optical measurements have been described previously [24]. The film resistivity was determined from the sheet resistance measurement by a four-point probe technique.

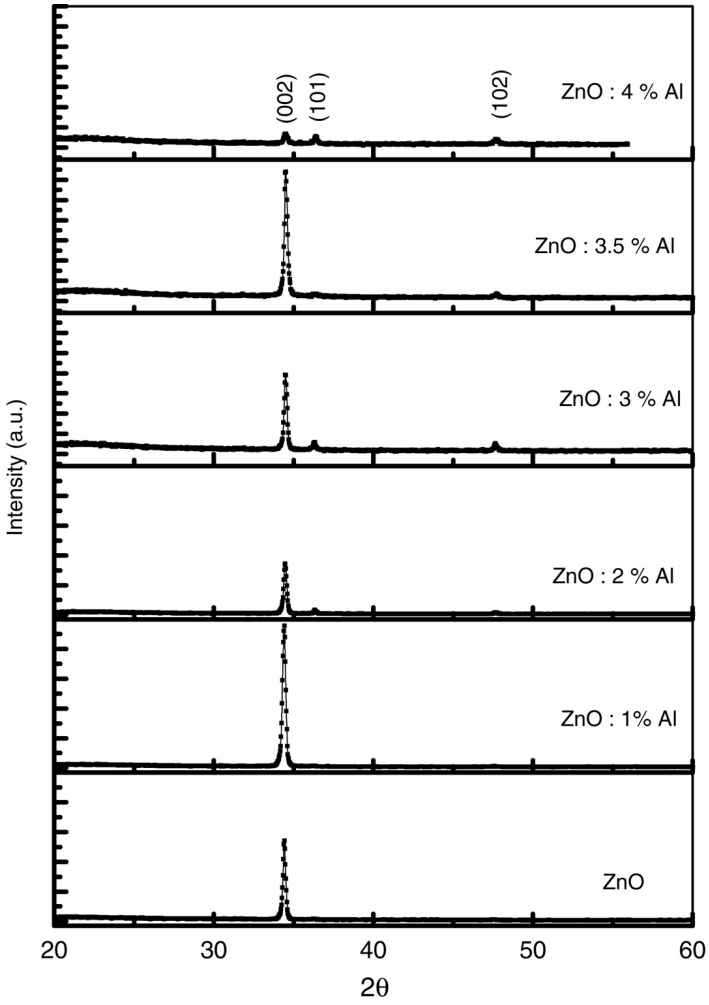

Fig. 1. XRD θ–2θ scan diagrams of undoped ZnO and AZO films deposited at 400 °C on quartz substrates for various Al doping concentrations.

3. Results and discussion

Fig. 1 shows the X-ray diffraction pattern of undoped ZnO and AZO films deposited at 400 °C on quartz substrates as a function of doping concentration. All films are polycrystalline with a hexagonal wurtzite-type structure. The undoped ZnO film have preferred (002) orientation. For samples with Al concentration higher than 2%, (101) and (102) reflection peaks of ZnO appear, thus indicating that Al causes a loss of preferential orientation of the films. Besides, for the sample with 4% the spectrum is of poor quality, and this indicates that Al doping causes a decrease of the crystalline quality of the films.

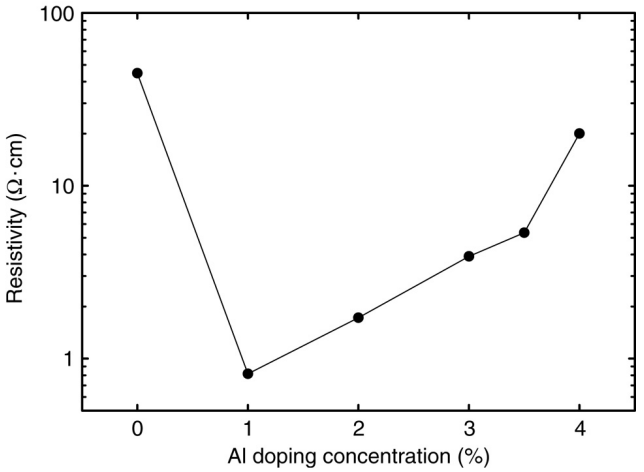

Fig. 2. Electrical resistivity of undoped ZnO and AZO films deposited on quartz substrate at 400 °C as a function of Al doping concentration.

This decrease in crystal quality may be due to the appearance of stress because of the difference in ion size between Zn ($r_{Zn^{2+}} = 0.074$ nm) and Al ($r_{Al^{3+}} = 0.054$ nm).

The electrical resistivity of AZO films as a function of the dopant concentration is plotted in Fig. 2. It initially decreases from 45 Ω cm in the undoped ZnO sample down to 0.8 Ω cm as the Al doping concentration increases up to 1%. This decrease in resistivity is due to the increase of the free carrier concentration as a result of electrons coming from the donor Al^{3+} ions incorporated as substitutional ions in Zn^{2+} cation sites or in interstitial positions [14]. However, after reaching a minimum value at 1% Al doping concentration, the resistivity increases with Al concentration up to 4%. The excess of Al doping seems to decrease the carrier concentration and/or carrier mobility in the film and consequently leads to an increase of the sheet resistivity. Several authors claim that excess of Al doping forms non-conducting Al_2O_3 clusters in the films, causing crystal disorder and producing defects which act as carrier traps rather than electron donors [25,26]. However, it is possible that the increase of Al doping can also cause a decrease in the crystal grain size, also affecting the mobility.

Fig. 3 shows optical transmittance spectra at room temperature for undoped ZnO and AZO films. All films exhibit a transmittance above 80%–90% along the visible range up to 750 nm and a sharp absorption onset at about 375 nm. All samples show a gap around 3.35 eV at room temperature. We have found no net increase of the bandgap with Al concentration due to the Burstein–Moss effect in our samples [27], except perhaps for 1% Al concentration. The decrease of the bandgap for samples with Al concentration higher than 1% is consistent with the increase of resistivity found in the samples with Al concentration larger than 1%. The lack of the Burstein–Moss effect in our highly doped samples suggests that the increase of resistivity in the doped samples above 1% Al concentration is due to a decrease in carrier concentration rather than to a decrease

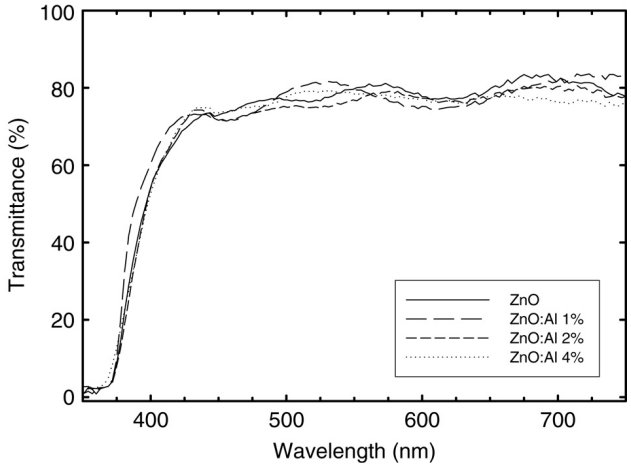

Fig. 3. Optical transmittance spectra at room temperature of undoped ZnO and several AZO films deposited on quartz substrate.

in carrier mobility. In this sense, an electron trap has been measured 0.44 eV below the conduction band in samples with 3% Al concentration [23].

Photoluminescence spectra obtained at 19 K for different ZnO films with different Al doping concentration are presented in Fig. 4. Undoped ZnO films show two emission peaks in the UV and green regions. The emission peaks are centred at 369 and 500 nm, respectively. The UV peak corresponds to emission due to bound excitons, while the green emission is mainly attributed to different intrinsic defects such as the zinc vacancy (V_{Zn}) and oxide antisite defects O_{Zn} forming local deep levels present in the bandgap [28,29]. AZO films do not show any emission similar to undoped samples. However, all Al-doped samples show a broad red emission band centred around 700 nm (1.77 eV) which is not present in undoped ZnO films. With the increase of the Al concentration, there is a blue shift of the red band and an increase of its intensity. Despite the intensity and width of the red band varying proportionally to the Al concentration in the samples, we think that this red emission band is probably not related to energy levels of Al in ZnO but to defects caused by the incorporation of Al into the ZnO lattice. The energy of the red band is around half the energy of the bandgap in ZnO, so we suggest that the Al doping promotes deep level defects causing the red emission. The small blue band around 410 nm (3 eV) present in our PL spectra is an artefact due to the undesired scattering of the laser onto the Al foil used to sustain samples inside the cryostat.

Fig. 5 shows the Raman scattering spectra in backscattering configuration of undoped ZnO and AZO samples grown over quartz. The undoped sample shows the usual modes observed in ZnO films: 330 cm^{-1} (E_2(high)–E_2(low)), 380 cm^{-1} (A_1(TO)), 440 cm^{-1} (E_2(high)), and 580 cm^{-1} (A_1(LO)). The A_1(LO) mode is hardly seen due to the weakening of LO modes by plasmon–phonon coupling [33]. This effect is usual in polar semiconductors with a high free-electron concentration, like ZnO and GaN. With an increase in Al doping, the E_2(high) and A_1(TO) modes decrease while the

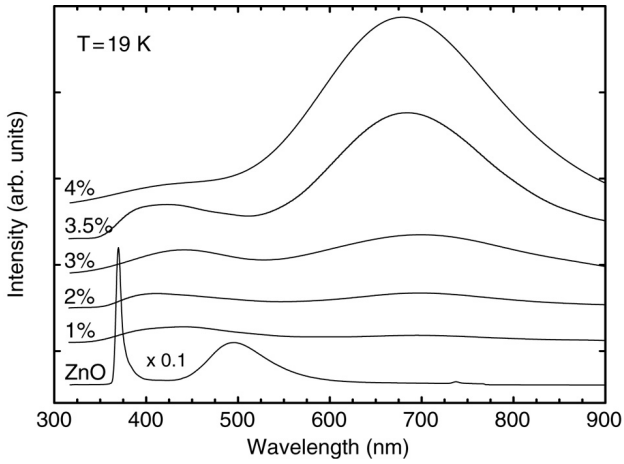

Fig. 4. Low-temperature photoluminescence spectra of as-grown undoped ZnO and AZO films deposited on quartz substrate for various Al doping concentrations.

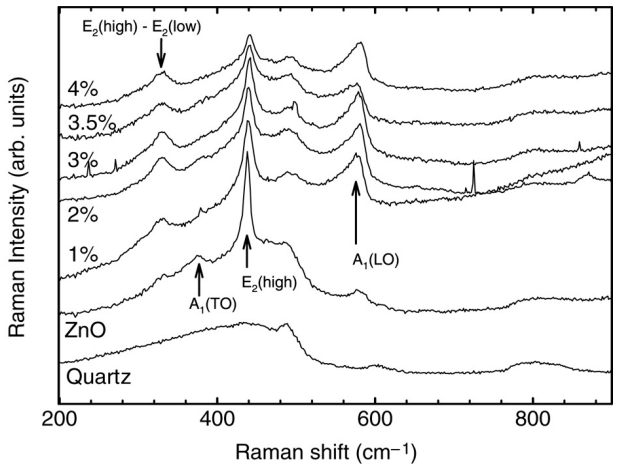

Fig. 5. Room-temperature Raman spectra of as-grown undoped ZnO and AZO films deposited on quartz substrate for various Al doping concentrations. A Raman spectrum of the quartz substrate is plotted for comparison.

E_2(high)–E_2(low) and the A_1(LO) modes increase. The increase of the 570 cm^{-1} mode has been observed in other AZO samples grown by radio-frequency magnetron sputtering [30] and attributed to the A_1(LO) or the silent B_1(high) mode observed by electric field induced (EFI) scattering, which causes an enhancement of Raman active phonons due to an increase of the electric field around grains that polarizes the field of excitonic states. We think that the asymmetric mode near 580 cm^{-1} can be attributed either to the A_1(LO) mode or to the silent B_1(high) mode. These modes could be observed by enhancement of Raman

active and inactive phonons by the change of the lattice symmetry due to disorder-activated Raman scattering (DARS) [31].

As regards undoped ZnO and AZO samples grown over Pt/quartz, optical microscopy has confirmed that they possess lower quality than those deposited directly on quartz. PL results (not shown here) indicate that even undoped ZnO/Pt/quartz samples show a small red band, which gives further support to its ascription to defect levels rather than to Al levels. As regards Raman scattering (not shown here) in undoped ZnO and AZO/Pt/quartz thin films, the signal is rather weak due to poor film quality, and it shows a broad band extending from 400 to 700 cm^{-1}. The E_2(high)–E_2(low) mode at 330 cm^{-1} and the E_2(high) mode at 437 cm^{-1} are very poorly observed on top of the broad band. Similar Raman spectra have been found for defect ZnO nanocrystals [24] and amorphous ZnO samples [32], so we attribute the Raman spectra of samples deposited onto Pt to undoped ZnO and AZO films which are partially amorphous, reflecting partially the one-phonon density of states.

4. Conclusions

Thin films of Al-doped ZnO oxide have been deposited onto quartz (and Pt/quartz) by spray pyrolysis. The samples are characterized by their transparency (more than 80% transmittance) and their resistivity. The smallest resistivity is found for a 1% Al concentration). No apparent changes in the band gap are triggered by increasing amounts of Al in the film. The samples are (002) preferentially oriented, although the orientation level lowers for increasing concentrations of Al. Doping with aluminium leads to the introduction of defects in the ZnO crystals. This has a profound effect on the corresponding Raman spectra, which indicates changes in the lattice symmetry and loss of crystalline quality in accordance with X-ray results. The photoluminescence of these AZO samples is rather different from that of the undoped films. Concretely, a very broad emission peak develops at around 700 nm, probably linked to the defects caused in the structure by the introduction of Al.

Acknowledgements

This work was supported by the European Union and MEC (Spain) through projects MAT2002-04539-C02-02, BQU2003-03737, and TEC2004-0051. R.G. is grateful to the SS.TT.II of the Universitat d'Alacant. J.R. Ramos-Barrado is grateful to the Junta de Andalucía through the research group FQM-192. The bursary holder, M.C. López, wishes to thank the MEC (Spain) and the CSIC (Spain).

References

[1] D.C. Look, Mater. Sci. Eng. B 80 (2001) 383.
[2] K. Vanheusden, C.H. Seager, W.L. Warren, D.R. Tallant, J. Caruso, M.J. Hampden-Smith, T.T. Kodas, J. Lumin. 75 (1997) 11.
[3] Y. Sanaka, H. Okuyama, S. Kijima, E. Kato, H. Noguchi, A. Ishibashi, Electron. Lett. 341 (1998) 1891.
[4] S. Nakamara, M. Senoh, S. Nagahama, N. Iwasa, T. Matsushita, T. Mukai, Proceedings of Second International Symposium on Blue Laser and Light Emitting Diodes, 1998, p. 371.

[5] D. Gorman, Photoluminescence and excitation studies, M.Sc. Thesis, Dublin City University, 2001 (unpublished).
[6] T. Soki, Y. Hatanaka, D.C. Look, Appl. Phys. Lett. 76 (2000) 3257.
[7] Z.K. Tang, G.K.L. Wong, P. Yu, M. Kawasaki, A. Ohtomo, H. Koinuma, Y. Segawa, Appl. Phys. Lett. 72 (1998) 3270.
[8] S. Cho, J. Ma, Y. Kim, Y. Sun, G.K.L. Wong, J.B. Ketterson, Appl. Phys. Lett. 75 (1999) 271.
[9] A. Mang, K. Reimann, St. Rübenacke, Solid State Commun. 94 (1995) 251.
[10] M.H. Sukkar, H.L. Tuller, Adv. Ceram. 7 (1984) 71.
[11] D.R. Lide, Handbook of Chemistry and Physics, 71st ed., CRC, Boca Raton, FL, 1991.
[12] D.C. Look, J.W. Hemsky, J.R. Sizelove, Phys. Rev. Lett. 82 (1999) 2552.
[13] J.H. Lee, B.O. Park, Thin Solid Films 426 (2003) 94.
[14] H. Kim, A. Pique, J.S. Horwitz, H. Murata, Z.H. Kafafi, C.M. Gilmore, D.B. Chresey, Thin Solid Films 377–378 (2000) 798.
[15] J.-H. Lee, B.-O. Park, Mater. Sci. Eng. B 106 (2004) 242.
[16] B.M. Ataev, A.M. Bagamadova, V.V. Mamedov, A.K. Omaev, M.R. Rabadanov, J. Cryst. Growth 198–199 (1999) 1222.
[17] D. Song, P.W. Denborg, W. Chin, A.G. Aberle, Sol. Energy Mater. Sol. Cells 73 (2002) 1.
[18] J.H. Lee, K.H. Ko, B.O. Park, J. Cryst. Growth 247 (2003) 119.
[19] A.V. Singh, M. Kumar, R.M. Mehra, A. Wakanaria, A. Yoshida, J. Indian. Inst. Sci. 81 (2001) 527.
[20] J. Cembrero, A. Elmanouni, B. Hartiti, M. Mollar, B. Marí, Thin Solid Films 451–452 (2004) 198.
[21] J.Y. Ma, S.C. Lee, J. Mater. Sci., Mater. Electron. 11 (2000) 35.
[22] R. Ayouchi, F. Martín, D. Leinen, J.R. Ramos-Barrado, J. Cryst. Growth 247 (2003) 497.
[23] R. Ayouchi, D. Leinen, F. Martín, M. Gabás, E. Dalchiele, J.R. Ramos-Barrado, Thin Solid Films 426 (2003) 68.
[24] B. Marí, J. Cembrero, F.J. Manjón, M. Mollar, R. Gómez, Phys. Status Solidi c 202 (2005) 1602.
[25] J. Hu, R.G. Gordon, J. Appl. Phys. 71 (1992) 880.
[26] A.F. Aktaruzzaman, G.L. Sharma, L.K. Malhotra, Thin Solid Films 198 (1991) 67.
[27] B.E. Sernelius, K.F. Berggren, Z.C. Jin, I. Hamberg, C.G. Granqvist, Phys. Rev. B 37 (1998) 10244.
[28] B. Lin, Z. Fu, Y. Jia, Appl. Phys. Lett. 79 (2001) 943.
[29] J. Wang, G. Du, Y. Zhang, B. Zhao, X. Yang, D. Liu, J. Cryst. Growth 263 (2004) 269.
[30] M. Tzolov, N. Tzenov, D. Dimova-Malinovska, M. Kalitzova, C. Pizzuto, G. Vitali, G. Zollo, I. Ivanov, Thin Solid Films 379 (2000) 28;
M. Tzolov, N. Tzenov, D. Dimova-Malinovska, M. Kalitzova, C. Pizzuto, G. Vitali, G. Zollo, I. Ivanov, Thin Solid Films 396 (2001) 274.
[31] F.J. Manjón, B. Marí, J. Serrano, A.H. Romero, J. Appl. Phys. 97 (2005) 053516.
[32] E.J. Ibanga, C. Le Luyer, J. Mugnier, Mater. Chem. Phys. 80 (2003) 490.
[33] B.H. Bairamov, A. Heinrich, G. Irmer, V.V. Toporov, E. Ziegler, Phys. Status Solidi b 119 (1983) 227.